Atmos. Meas. Tech. Discuss., https://doi.org/10.5194/amt-2018-348
Manuscript under review for journal Atmos. Meas. Tech.
Discussion started: 11 December 2018

Atmospheric Measurement Techniques Discussions

Studies of the horizontal inhomogeneities in NO_2 concentrations above a shipping lane using ground-based MAX-DOAS and airborne imaging DOAS measurements

André Seyler[1], Andreas C. Meier[1], Folkard Wittrock[1], Lisa Kattner[1,2], Barbara Mathieu-Üffing[1,2,a], Enno Peters[1,b], Andreas Richter[1], Thomas Ruhtz[3], Anja Schönhardt[1], Stefan Schmolke[2], and John P. Burrows[1]

[1]Institute of Environmental Physics, University of Bremen, Germany
[2]Federal Maritime and Hydrographic Agency (BSH), Hamburg, Germany
[3]Institute for Space Sciences, Freie Universität Berlin, Germany
[a]now at: State Agency for Agriculture, Environment and Rural Areas Schleswig-Holstein (LLUR), Germany
[b]now at: Institute for the Protection of Maritime Infrastructures, German Aerospace Center (DLR), Bremerhaven, Germany

Correspondence to: André Seyler (aseyler@iup.physik.uni-bremen.de)

Abstract.

This study describes a novel application of an "onion peeling" like approach to MAX-DOAS measurements of shipping emissions aiming at investigating the strong horizontal inhomogeneities in NO_2 over a shipping lane. To monitor ship emissions on the main shipping route towards the port of Hamburg, a two-channel (UV and visible) MAX-DOAS instrument was deployed on the island Neuwerk in the German Bight, 6–7 km south of the main shipping lane. Utilizing the fact that the effective light path length in the atmosphere depends systematically on wavelength, simultaneous measurements and DOAS retrievals in the UV and visible spectral range are used to probe air masses at different horizontal distances to the instrument to estimate two-dimensional pollutant distributions. Two case-studies have been selected to demonstrate the ability to derive the approximate plume positions in the observed area. A situation with northerly wind shows high NO_2 concentrations close to the measurement site and low values in the north of the shipping lane. The opposite situation with southerly wind, unfavorable for the on-site in situ instrumentation, demonstrates the ability to detect enhanced NO_2 concentrations several kilometers away from the instrument. To validate the approach, a comparison to air-borne imaging DOAS measurements during the NOSE campaign in July 2013 is performed, showing good agreement between the approximate plume position derived from the onion peeling MAX-DOAS and the air-borne measurements. Combining synergistically information about the plume width from the air-borne measurements and about the vertical plume extent from MAX-DOAS, yields NO_2 concentrations in the plume from both measurements which agree very well.

1 Introduction

Over the last decades, there has been a strong increase in ship traffic and shipping emissions of gas phase pollutants but a reduction in their land sources in much of Europe. This has lead to an increasing contribution of shipping emissions to

Atmos. Meas. Tech. Discuss., https://doi.org/10.5194/amt-2018-348
Manuscript under review for journal Atmos. Meas. Tech.
Discussion started: 11 December 2018

Atmospheric Measurement Techniques Discussions

air pollution in coastal regions. Consequently, emission reduction measures such as lowering the allowed sulfur content in shipping fuel according to MARPOL VI (IMO, 2008) have been enacted in many places including the North Sea and the Baltic Sea. In order to monitor the effectiveness of these measures as well as the overall impact of ship emissions on air quality, measurements of air pollution from ships are required.

Most measurements of pollution are performed with in-situ instrumentation, and this includes monitoring of the effect of ship emissions. As shown in Seyler et al. (2017), MAX-DOAS measurements can provide both a complementary approach and an alternative to in-situ trace gas measurements at sites, where the ships are several kilometers away from the instrument and interpretation of in-situ measurements is challenging due to dilution and broadening of the plume during the travel time from the ships to the measurement site.

MAX-DOAS measurements pointing at the horizon probe a long horizontal light path and are thus very sensitive to absorbers located close to the ground. The strong wavelength dependence of Rayleigh scattering ($\propto \lambda^{-4}$) leads to longer effective horizontal light paths for longer wavelengths. Simultaneous measurements and DOAS retrievals in the UV and visible spectral range can thus be used to probe different parts of the horizontal light path, an approach which is often called "onion peeling" method and has been applied to MAX-DOAS measurements before: Ortega et al. (2015) used this method to retrieve two dimensional NO_2 fields from circular azimuth scans around the instrument in the framework of the MAD-CAT campaign (Multi-Axis DOAS Comparison campaign for Aerosols and Trace gases) in Mainz, Germany. The aim of the study was the investigation of horizontal gradients in a strongly polluted urban area, with the cities of Mainz, Wiesbaden and Frankfurt as well as the Frankfurt airport close by, focussing on comparison to satellite measurements.

The present study focuses on measurements in a relatively clean coastal region where ships passing by the island are often the only dominant source of air pollution (Seyler et al., 2017). The ships are mobile point sources of NO_x emissions and the emitted exhaust gas plumes are transported, depending on wind conditions, leading to a strongly inhomogeneous NO_2 field over the shipping lane.

Ortega et al. (2015) probed a circular area with 14 azimuthal viewing directions distributed over a 360° view around the instrument. In the present study, a similar measurement pattern was applied using 5 different azimuth directions distributed over a 120° angle to cover the shipping lane close to the island (see Fig. 1b) with sufficient time resolution to monitor individual passing ships. The onion peeling approach provides additional distance information for the measured NO_2 columns.

This study uses measurements in both the UV (∼350 nm) and blue spectral range (∼450 nm), while Ortega et al. (2015) used additional measurements in the yellow spectral range (∼570 nm) to get an even longer effective horizontal light path and cover a larger region. This is not possible here as the instrument used has a smaller wavelength coverage.

As can be seen from Fig. 1a and b, the measurement site on the island Neuwerk is ideal for applying this measurement principle: The distance between site and shipping lane is on the order of 6 to 10 kilometers, depending on the azimuthal viewing direction, which is in the range of typical UV horizontal effective light path lengths (Seyler et al., 2017). Depending on the azimuthal direction, the additional probing distance gained by measurements in the visible spectral range covers the shipping lane or the region in the north of the ship track. As it is shown in the following, this enables the NO_2 distribution

caused by the ship emission plumes over and around the ship track to be determined. In addition even the distance and course of the emitted plumes is observed.

This publication is a follow up to an earlier study entitled "Monitoring shipping emissions in the German Bight using MAX-DOAS measurements" (Seyler et al., 2017) where long-term measurements were used to asses the impact of shipping emissions on the regional air quality, while the present study focuses on describing, demonstrating and validating a new method for improved measurements of ship emissions and their localization.

The present study is part of the project MESMART (measurements of shipping emissions in the marine troposphere), a cooperation between the University of Bremen (Institute of Environmental Physics, IUP) and the German Federal Maritime and Hydrographic Agency (Bundesamt für Seeschifffahrt und Hydrographie, BSH), supported by the Helmholtz Zentrum Geesthacht. For further information visit http://www.mesmart.de/.

2 Measurement site and instrumentation

2.1 MAX-DOAS instrument

The multi axis differential optical absorption spectroscopy (MAX-DOAS) (Hönninger et al., 2004; Wittrock et al., 2004) is a well-established technique for measurements of trace gases that absorb in the UV and visible spectral range. This passive remote sensing method measures spectra of scattered sunlight in multiple viewing directions and is highly sensitive to absorbers in the atmospheric boundary layer. A two-channel MAX-DOAS instrument was deployed on the island Neuwerk from July 2013 to July 2016. It comprises a telescope unit with a field of view of 1° on a pan-tilt head, an optical fiber cable and two spectrometers with CCD cameras for UV (304.6–371.7 nm) and visible (398.8–536.7 nm) spectral range. This arrangement is optimized for the simultaneous retrieval of NO_2 and O_4 in both spectral domains.

A detailed description of the MAX-DOAS instrument and its components as well as the general measurement geometry for ship emission measurements is given in Seyler et al. (2017). Details of the DOAS fit settings used are given in Table 1.

2.2 Measurement site

Neuwerk is a small island in the German Bight, northwest of the city of Cuxhaven at the mouth of the river Elbe, around 9 kilometers off the coast. An overview of the area is shown in Fig. 1a. The main shipping lane into the river Elbe towards the port of Hamburg passes the island in the north in a distance of 6–7 km (see Fig. 1a). The MAX-DOAS instrument was installed on a radar tower in a height of 30 meters above ground level. Additional instrumentation on site included in situ gas analyzers (NO_x, SO_2, O_3, CO_2) in a combined compact housing (Airpointer from MLU-recordum, Austria), a Davis Vantage Pro 2 semi-professional weather station and an automatic identification system (AIS, (IMO, 2002)) receiver. The AIS signal broadcasts various information like identification, position, speed, course and size of the ship. Broadcasting equipment is mandatory for all ships larger than 20 m. In the present study, the AIS information is used to attribute the measurements to

Atmos. Meas. Tech. Discuss., https://doi.org/10.5194/amt-2018-348
Manuscript under review for journal Atmos. Meas. Tech.
Discussion started: 11 December 2018

Atmospheric Measurement Techniques Discussions

Table 1. DOAS fit settings for the retrieval of NO_2 and O_4 in UV and visible spectral range

Parameter	NO_2 (UV)	NO_2 (visible)
Fitting window	338–370 nm	425–497 nm
Polynomial degree	4	3
Intensity offset	Constant	Constant
Zenith reference	Coinciding zenith measurement*	Coinciding zenith measurement*
SZA limit	Up to 85° SZA	Up to 85° SZA
O3	223 K & 243 K (Serdyuchenko et al., 2014)	223 K (Serdyuchenko et al., 2014)
NO_2	298 K (Vandaele et al., 1996)	298 K (Vandaele et al., 1996)
O_4	293 K (Thalman and Volkamer, 2013)	293 K (Thalman and Volkamer, 2013)
H2O	–	293 K (Lampel et al., 2015)
HCHO	297 K (Meller and Moortgat, 2000)	–
Ring	SCIATRAN (Rozanov et al., 2014)	SCIATRAN (Rozanov et al., 2014)

* Interpolation in time between the zenith measurements directly before and after the off-axis scan.

individual ships. Wind direction and speed is available with a time resolution of 10 minutes from two stations (see Fig. 1a), one on Neuwerk and one on the neighboring island Scharhörn, operated by the Hamburg Port Authority (HPA).

To sample a larger region, the MAX-DOAS was set up to have five different azimuthal viewing directions: 310°, 335°, 5°, 35° and 65° with respect to north, each pointing towards different sections of the shipping lane (see Fig. 1b).

For further information on the measurement site and instrumentation see Seyler et al. (2017).

3 Methodology

The quantity retrieved from DOAS measurements is the concentration of an absorber integrated along the atmospheric light path, the so-called slant column density (SCD). To measure the NO_2 absorption inside the ship plumes emitted on the shipping lane, the instrument is pointing in 0.5° elevation towards the horizon. Taking a close-in-time zenith-sky measurement as a reference, in a first assumption only the absorption along the horizontal part of the effective light path is retrieved and the absorption higher up in the atmosphere cancels out. This yields the differential slant column density (DSCD).

For the comparison with in situ measurements the MAX-DOAS horizontal trace gas columns are converted to horizontal path averaged volume mixing ratios (VMR) by using the O_4 scaling approach (see Section 3.1). The onion peeling approach (see Section 3.2) is used to separate NO_2 absorptions at different horizontal distances to derive separate NO_2 VMRs and estimate the distance to the plumes.

Atmos. Meas. Tech. Discuss., https://doi.org/10.5194/amt-2018-348
Manuscript under review for journal Atmos. Meas. Tech.
Discussion started: 11 December 2018

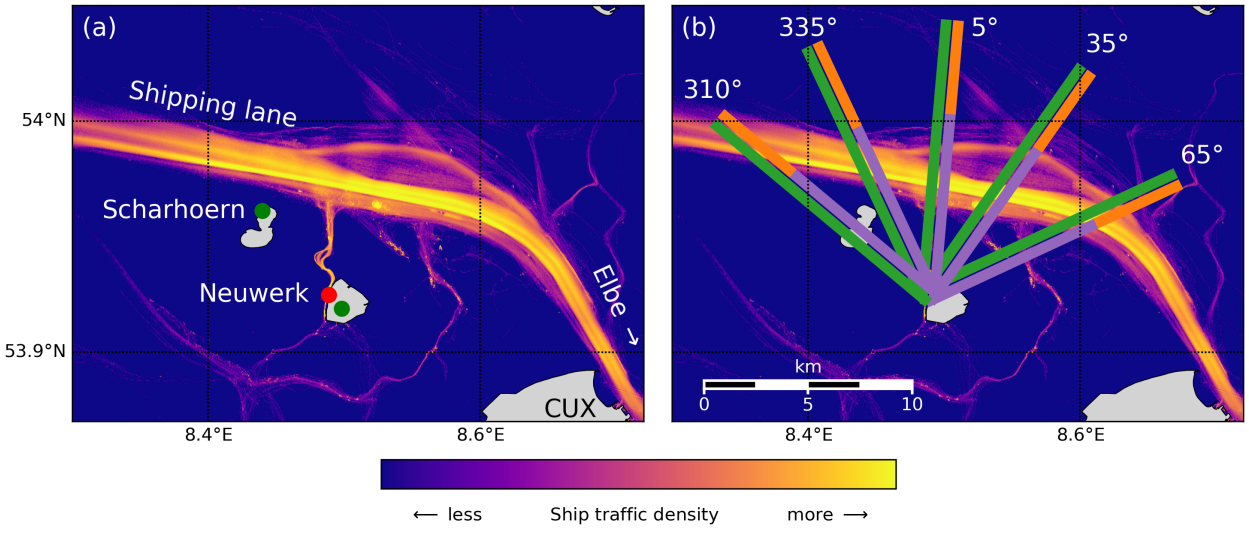

Figure 1. (a) Ship traffic density map calculated from all received AIS messages (2013-2016) showing the main shipping lane from the North sea into the Elbe river close to the measurement site on a radar tower on the island Neuwerk (red dot). Wind measurements are available on Neuwerk as well as the neighbouring island Scharhörn (green dots). (b) Effective horizontal light paths in UV (purple line) and visible spectral range (green line) for the five azimuthal viewing directions of the MAX-DOAS instrument (310°, 335°, 5°, 35°, 65°, with respect to north), shown for typical light path lengths of 9 km (UV) and 13 km (vis), respectively. The difference between both paths, ΔL, is highlighted by the orange line.

3.1 O_4 scaling approach – methodology and limitations

The oxygen collision complex O_4 absorbs in similar wavelength ranges as NO_2 in the UV and visible. Since the near-surface concentration of O_4 is known, the effective horizontal path length can be calculated by dividing the DSCD of O_4 by its number density n_{O_4}:

$$L = \frac{\mathrm{SCD}_{O_4,\mathrm{horiz}} - \mathrm{SCD}_{O_4,\mathrm{zenith}}}{n_{O_4}} = \frac{\mathrm{DSCD}_{O_4}}{n_{O_4}}$$

with $n_{O_4} = (n_{O_2})^2$, which can be calculated from the measured temperature and pressure. This can be done independently for both UV and visible measurements, giving average light path lengths of $L_{\mathrm{UV}} = (9.3 \pm 2.3)\,\mathrm{km}$ and $L_{\mathrm{vis}} = (12.9 \pm 4.5)\,\mathrm{km}$ [mean $\pm$ standard deviation] for the three years of measurements on Neuwerk, depending on the observational conditions. Under clear sky conditions, typical light path lengths are 10 km in the UV and 15 km in the visible spectral range (Seyler et al., 2017).

Knowing the horizontal light path length L, the NO_2 DSCD can be divided by L to obtain the average concentration (number density) of NO_2 along the horizontal light path. Dividing the NO_2 concentration by the concentration of air, n_{air}, which can be

Atmos. Meas. Tech. Discuss., https://doi.org/10.5194/amt-2018-348
Manuscript under review for journal Atmos. Meas. Tech.
Discussion started: 11 December 2018

calculated via the ideal gas law from the measured temperature and pressure, yields the average volume mixing ratio (VMR) along L:

$$\mathrm{VMR}_{\mathrm{NO_2}} = \frac{\mathrm{SCD}_{\mathrm{NO_2,horiz}} - \mathrm{SCD}_{\mathrm{NO_2,zenith}}}{L \cdot n_{\mathrm{air}}} = \frac{\mathrm{DSCD}_{\mathrm{NO_2}}}{L \cdot n_{\mathrm{air}}}$$

This $\mathrm{O4}$ scaling approach has been successfully applied to MAX-DOAS measurements before, for example in urban polluted areas (Sinreich et al., 2013; Wang et al., 2014) or at high mountain sites (Gomez et al., 2014; Schreier et al., 2016).

For a homogeneous, well-mixed $\mathrm{NO_2}$ field along the light path, this VMR must agree with in situ measurement from the same altitude. For the ship emission case, where emission plumes are filling only a small fraction of the several kilometers long light path, the path-averaged MAX-DOAS VMR will not represent the VMR inside the plume and values will be smaller than in situ measurements inside the plume (Seyler et al., 2017).

However, the different shapes of the atmospheric profiles of $\mathrm{NO_2}$ (emitted and formed close to the surface) and $\mathrm{O_4}$ (exponentially decreasing with altitude) introduce systematic errors as has been shown by Sinreich et al. (2013) and Wang et al. (2014). To account for this, correction factors calculated by radiative transfer simulations are needed. These depend on well-known quantities such as solar zenith angle (SZA) and relative solar azimuth angle (RSAA) as well as on unknown quantities such as aerosol optical density (AOD), height of the $\mathrm{NO_2}$ box profile and the extent and vertical position of the aerosol layer relative to the $\mathrm{NO_2}$ profile (Sinreich et al., 2013), which are not measured and cannot be easily approximated for the present study. In previous studies, it has been assumed that $\mathrm{NO_2}$ is well mixed within a layer from the surface up to a top layer height and absent above this altitude. This is not a valid assumption in case of horizontally inhomogeneous $\mathrm{NO_2}$ fields such as those probed over the shipping lane. As in Seyler et al. (2017), scaling factors are therefore not considered here, presumably leading to a systematic overestimation of path lengths and thus underestimation of MAX-DOAS VMRs (Sinreich et al., 2013; Wang et al., 2014).

3.2 "Onion peeling" MAX-DOAS approach

As mentioned above, the wavelength dependence of Rayleigh scattering results in a wavelength dependence of the light path lengths after the last scattering point. This can be utilized to probe different air masses in the atmosphere by measuring both in the UV and visible spectral range.

The aforementioned $\mathrm{O_4}$ scaling method gives two path-averaged volume mixing ratios for each measurement; one for the shorter UV and one for the longer visible effective horizontal light path, which are shown in Fig. 1b and 2 as a purple and green line, respectively. One can calculate a third volume mixing ratio from the difference of the two DSCDs and path lengths:

$$\mathrm{VMR}_{@\Delta L} = \frac{\mathrm{DSCD}_{\mathrm{vis}} - \mathrm{DSCD}_{\mathrm{UV}}}{(L_{\mathrm{vis}} - L_{\mathrm{UV}}) \cdot n_{\mathrm{air}}} = \frac{\Delta\mathrm{DSCD}}{\Delta L \cdot n_{\mathrm{air}}} \quad (1)$$

This yields the average volume mixing ratio $\mathrm{VMR}_{@\Delta L}$ along the path difference ΔL, which is shown as an orange line in Fig. 1b and 2.

Atmos. Meas. Tech. Discuss., https://doi.org/10.5194/amt-2018-348
Manuscript under review for journal Atmos. Meas. Tech.
Discussion started: 11 December 2018

Atmospheric Measurement Techniques Discussions

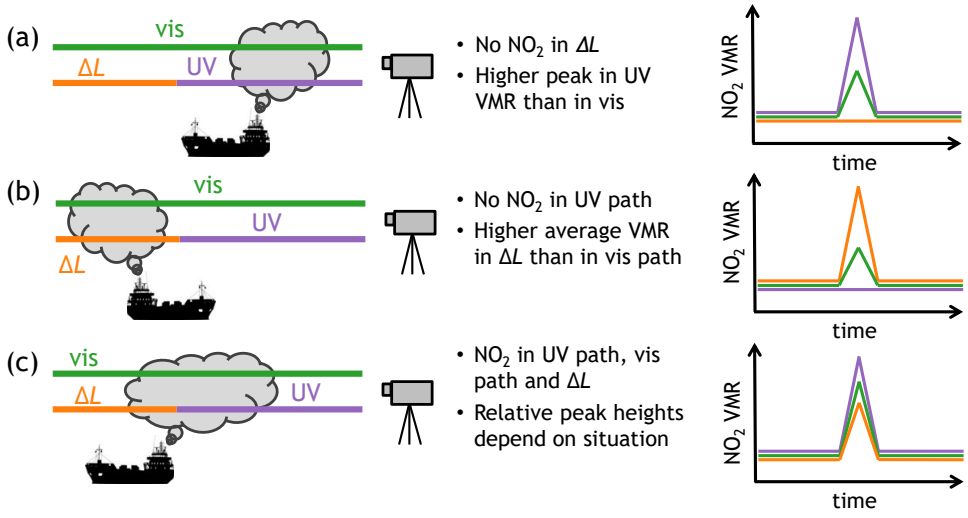

Figure 2. Plume–light-path geometry and the resulting path averaged NO_2 concentrations for three possible cases: When the plume is close to the instrument and completely covered by the UV path (a), when the plume is further away from the instrument than the UV scattering point and is only covered by the visible path (and ΔL) (b) and when the plume is located around the UV scattering point (c)

As each ship is a moving point source for NO_2 emissions, the NO_2 field over a shipping lane is strongly inhomogeneous. This means that the NO_2 is in general not distributed evenly along any of the effective horizontal light paths.

Depending on the position of the plume in relation to the UV and visible light path, the path averaged mixing ratios can differ substantially. Figure 2 shows schematically the plume-light-path geometry for three possible observation scenarios and illustrates the expected NO_2 signal for the different horizontal light paths.

In case (a) the plume is close to the instrument and is completely covered by the shorter UV path L_{UV}, i. e. it is closer to the instrument than the (mean) last scattering point in the UV. Although both paths cover the same amount of NO_2, the retrieved path-averaged concentration is higher for the UV signal because of the higher relative contribution of the fraction of the light path which probes the NO_2 plume. The path difference ΔL incorporates no NO_2 from the emission plume, resulting in zero or background level NO_2 from there. It can be seen from Fig. 1b that this situation occurs for northerly wind directions. Section 4.2 shows example measurement results for such a case.

Case (b) shows the opposite situation, when the plume is further away from the instrument than the UV scattering point and only covered by the visible path L_{vis}. This results in an enhanced signal for the NO_2 retrieved in the visible, and no signal in the UV. The path averaged concentration retrieved for ΔL is even higher, because ΔL is only a segment of the visible path and therefore shorter than the complete visible path. On Neuwerk, such a situation can occur for southerly winds (compare Fig. 1b). Section 4.3 shows example measurement results for this kind of situation.

In case (c) the plume is close to the UV scattering point. All three light paths see enhanced NO_2. The relative peak heights depend on the fraction of plume NO_2 probed by the different light paths as well as the total light paths lengths. Situations like this will most likely occur for westerly and easterly winds.

As already discussed in Seyler et al. (2017), the measured column density as well as the path-averaged concentration do not only depend on the emitted amount of NO_2 inside the plume, but also on the angle of intersection between plume and line of sight of the instrument. The smallest absorptions, and thus column amounts, will be retrieved if the plume runs orthogonal to the line of sight, the highest values if the instrument measures along the plume. The latter can occur for certain combinations of wind direction, wind speed and ship movement direction and speed. Because of the movement of the ships (and the shape of the shipping lane), this is in general not the case when the instrument measures in wind direction, as it would be for a stationary point source.

The time span between plume emission and measurement is also important for the measured NO_2 values because of NO to NO_2 titration, as a large fraction of nitrogen oxides (NO_x) is emitted as NO (Alföldy et al., 2013; Zhang et al., 2016), which does not absorb in the spectral range covered and cannot be measured with MAX-DOAS. Therefore, the NO_2 signal increases with distance from the ship and, depending on the wind direction, with distance from the ship track.

3.3 Plume trajectories

Here, plume trajectories have been calculated as simple forward trajectories on a 10 s time grid, where each point shaped plume air parcel on each time step is moved from its old position to a new position, depending on wind direction and speed. Each ship emits a new plume air parcel at each time step at the actual ship position. By starting with an initialization period of 90 minutes before the measurements, old plumes from ships that passed by the island before and already left the map can be included in maps as those shown in Fig. 6. The width of the schematic plumes in the maps is not to scale and depends simply on the ship size, with broader plumes drawn for larger ships. Plume broadening and dilution over time is neglected. However, the gray shading of the drawn plumes gets brighter with each time step to indicate the plume age. The trajectories are two-dimensional, vertical wind components were not measured and are therefore neglected. While some weather models provide such vertical wind components, their spatial and time resolution is too low for this application.

4 Results

4.1 Onion peeling approach applied to ship emission measurements

Figure 3 shows the measured NO_2 DSCDs in 0.5° elevation for the 335° azimuth direction (compare Fig. 1b) on 26 May 2014. The NO_2 shows sharp peaks, which originate from shipping emissions, with rapid changes of NO_2 levels between consecutive measurements of up to one order of magnitude. The small, but non-zero baseline between the peaks shows an ambient NO_2 pollution, which is enhanced in the morning hours. The background NO_2 signal may be originating from land-based sources

Atmos. Meas. Tech. Discuss., https://doi.org/10.5194/amt-2018-348
Manuscript under review for journal Atmos. Meas. Tech.
Discussion started: 11 December 2018

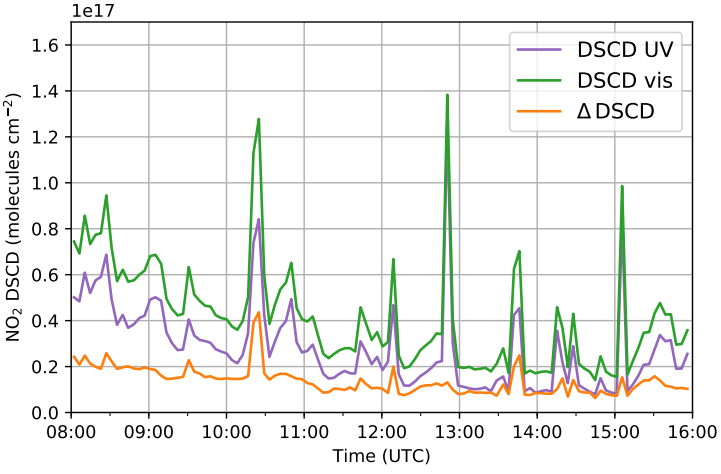

Figure 3. Differential slant column densities of NO_2 on 26 May 2014 in 0.5° elevation and 335° azimuth for the UV (purple) and visible spectral range (green) and their difference (orange)

but may also contain residual, diluted shipping emissions. The morning enhancement might be due to the morning traffic rush hour or boundary layer height changes.

As a result of the longer light path, the NO_2 columns measured in the visible range are larger than in the UV. The difference between visible and UV columns, ΔDSCD, shows concurrent peaks for some of the peaks, with varying relative height. The peak at 12:50 UTC is not visible in the ΔDSCD, indicating that the plume must be closer to the instrument than the UV scattering point.

Figure 4 shows the corresponding effective horizontal light path lengths derived from the measured O_4 DSCDs. For a clear sky day like this, path lengths are quite constant over time. Clouds can decrease or increase the light path length (and O_4 absorption) by multiple scattering, depending on the cloud's position and its optical properties, especially its optical thickness (Wagner et al., 2014). As a result, a day with scattered or broken clouds will show much more variation in path lengths even between consecutive measurements by having clouds in either off-axis or reference measurement or both or neither, which makes interpretation of results more difficult.

Figure 5 shows the horizontal path averaged NO_2 volume mixing ratios retrieved from the NO_2 DSCDs by using the O_4 scaling approach with the path lengths for UV and visible shown in Fig. 4, as well as the volume mixing ratio on the path difference calculated via Eq. 1. The baselines of all three curves agree very well, showing that the ambient NO_2 background pollution is well-mixed in the boundary layer and homogeneously distributed along all light paths sections. However, the sharp peaks originating from ship emission plumes have different relative heights, showing that the corresponding NO_2 field is inhomogeneous. The strong NO_2 signal at 12:50 UTC without enhanced NO_2 VMR on the path difference, resembling situation (a) in Fig. 2, will be further investigated in the next section.

Atmos. Meas. Tech. Discuss., https://doi.org/10.5194/amt-2018-348
Manuscript under review for journal Atmos. Meas. Tech.
Discussion started: 11 December 2018

Atmospheric Measurement Techniques Discussions

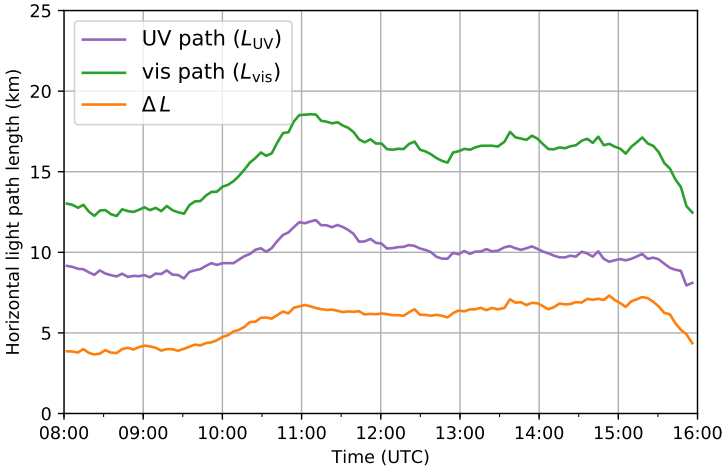

Figure 4. Effective horizontal light path lengths on 26 May 2014 in 0.5° elevation and 335° azimuth for UV (purple) and visible spectral range (green) and their difference (orange)

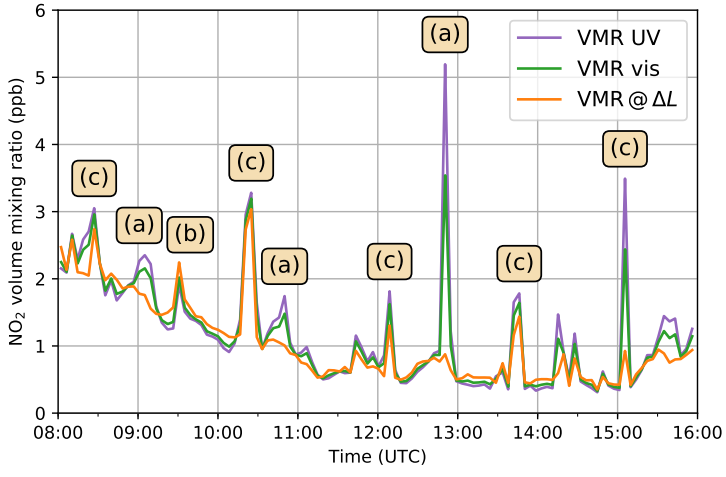

Figure 5. Horizontal path averaged volume mixing ratios of NO_2 on 26 May 2014 in 0.5° elevation and 335° azimuth for the UV (purple) and visible path (green) as well as for the path difference ΔL (orange). The yellow labels over the peaks indicate the respective situation from Fig. 2.

Atmos. Meas. Tech. Discuss., https://doi.org/10.5194/amt-2018-348
Manuscript under review for journal Atmos. Meas. Tech.
Discussion started: 11 December 2018

4.2 Northerly wind situations

For northerly winds, the pollution plumes emitted from the ships are blown towards the radar tower, resulting in enhanced NO_2 concentrations south of the shipping lane (compare Fig. 1b). In the north of the shipping lane, concentrations should be low, resembling situation (a) in Fig. 2.

In Fig. 6, a 12 minute sequence of consecutive MAX-DOAS measurements on 26 May 2014 starting at 12:46 UTC (14:46 local time) is shown for more detailed investigation of the strong NO_2 signal already seen in Fig. 5 at 12:50 UTC. Plotted in each map are the length and location of the UV path and ΔL as colored lines, with color representing the respective path averaged NO_2 VMR. In situ NO_2 VMRs are shown as colored dots at the measurement site. Shown are also ship positions and course from AIS data, plume trajectories (see Section 3.3) and wind speed and direction.

The sequence of maps shows two ships (magenta triangles) on the shipping lane, moving in opposite directions. The larger ship (length 351 m) moves westward, the smaller ship (length 151 m) moves eastward. The locations of the two plumes (gray shaded stripes) differ considerably due to the different movement directions of the ships and the curved shape of the shipping lane around the island.

In the first panel, the MAX-DOAS measurements at 12:46:24 UTC in 335° azimuth direction are shown. The horizontal path averaged NO_2 VMRs are low (< 1 ppb NO_2) and agree very well between the different path segments as well as with the in situ measurements, showing that the ambient background NO_2 is homogeneously well-mixed in the boundary layer. The fact that the plume from the smaller ship shows up only slightly in the measurements can have two possible reasons: Either the in-plume NO_2 concentrations are rather low or the plume is in the wrong height and not in the observed air volume along the line of sight of the instrument, which due to the 1°field of view is quite narrow close to the instrument.

Panels 2 to 4 (5°, 35° and 65° azimuth, respectively) show enhanced NO_2 VMRs (up to 4 ppb) along the UV path close to the instrument, likely due to the plume of the big ship, and low VMRs along ΔL further away from the instrument. Although MAX-DOAS measurements show enhanced NO_2 between site and UV scattering point the plume has not reached the radar tower yet and in situ values therefore stay low.

Panel 5 shows the measurements in the 310° viewing direction which are similar to the measurements in 335° azimuth angle in Panel 1.

In Panels 6 to 10, the plume approaches the radar tower and in situ values begin to rise. MAX-DOAS VMRs are again high close to the radar tower and low in the north of the shipping lane. Due to different angles of intersection between plume and line of sight, the MAX-DOAS path averaged UV VMR is different, showing the highest value of ~ 5 ppb when measuring alongside the plume (Panel 6) and much lower values when measuring orthogonally to it (e.g. Panel 3). Starting with Panel 9 the in situ values are even higher, with more than 5 ppb, which is not represented in the figure as the color scale is saturated. This is because the in situ instrument measures directly the NO_2 VMR inside the plume and the MAX-DOAS delivers only path-averaged values, which underestimate the local VMR inside the plume.

Atmos. Meas. Tech. Discuss., https://doi.org/10.5194/amt-2018-348
Manuscript under review for journal Atmos. Meas. Tech.
Discussion started: 11 December 2018

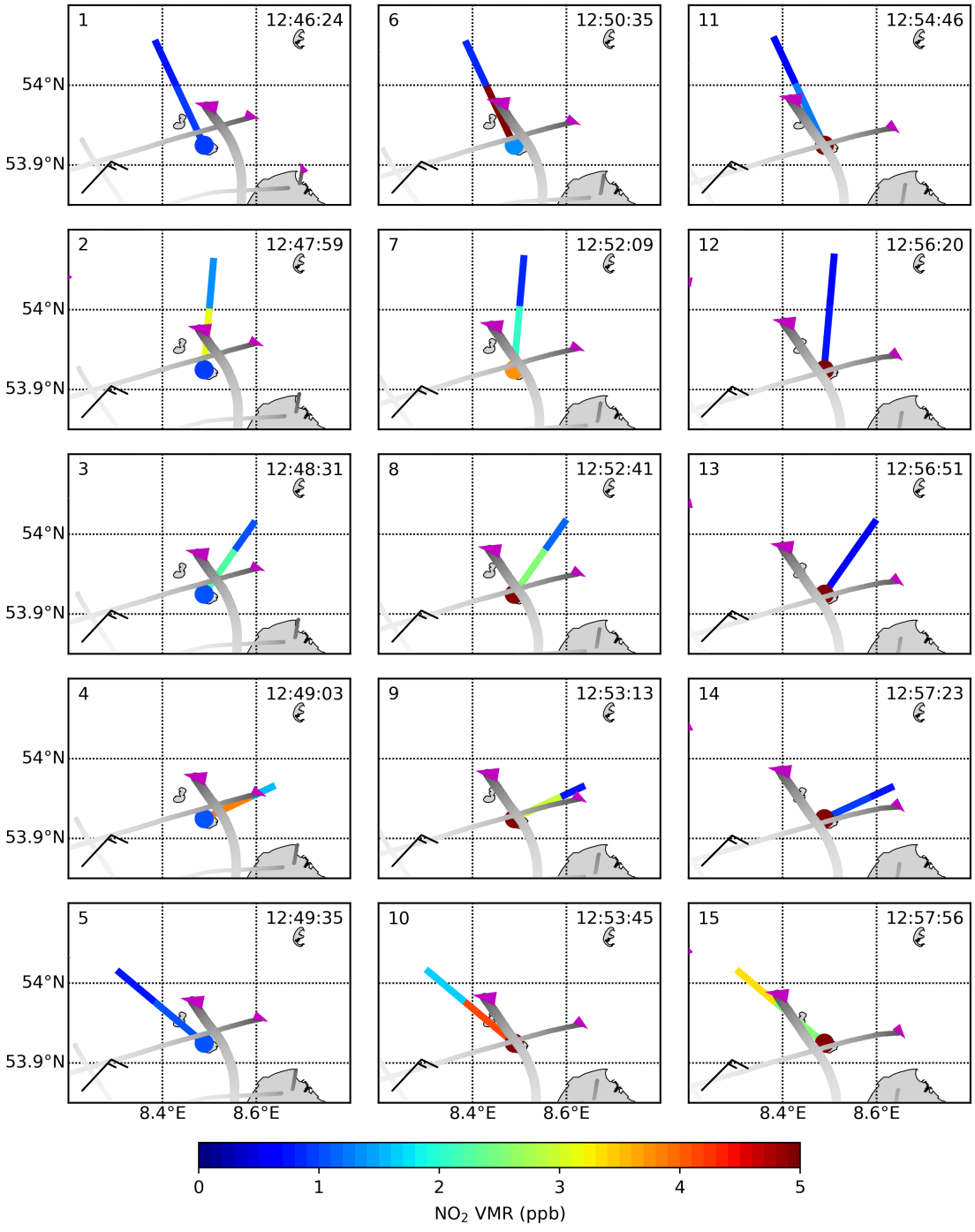

Figure 6. Sequence of maps showing 15 consecutive measurements in 0.5° elevation on 26 May 2014, starting at 12:46 UTC (14:46 local time): The extent of the UV path and ΔL and corresponding path averaged NO_2 VMRs are shown as colored lines. In situ NO_2 VMRs are shown as a colored dot at the location of the measurement site. Magenta triangles show the ship position and course (sharp tip), with larger triangles for larger ships. Grey point clouds show forward trajectories of the emission plumes calculated from wind speed and direction for the moving ship. Wind direction and speed is shown with meteorological wind barbs.

Atmos. Meas. Tech. Discuss., https://doi.org/10.5194/amt-2018-348
Manuscript under review for journal Atmos. Meas. Tech.
Discussion started: 11 December 2018

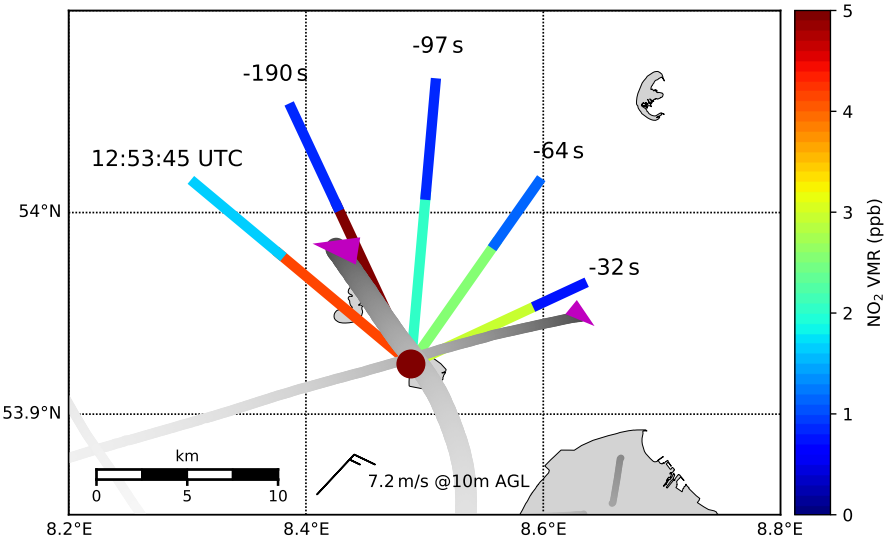

Figure 7. Map showing a zoom in onto Panel 10 of Figure 6 and the four previous MAX-DOAS measurementsobservations, being measured between 30 seconds and 3 minutes before the current observation. Horizontal light path lengths (UV path and ΔL) and corresponding path averaged volume mixing ratios of NO_2 are shown as colored lines, in situ NO_2 values as a colored dot at the location of the instrument. Magenta triangles show the ship position and course, with larger triangles for larger ships. Gray stripes show forward trajectories of the emission plumes calculated from wind speed and direction for the moving ship. Please keep in mind that ship and plume position were different for the past measurements. Wind direction and speed is shown with a meteorological wind barb.

In Panel 11 the ship plume has moved out of the narrow line of sight of the MAX-DOAS instrument and measured NO_2 values drop rapidly to ambient concentrations on all lightboth path segments. Panels 11 to 14 show all low MAX-DOAS measurements, while the plumes of both ships are hitting the radar tower leading to a very high in situ signal.

In Panel 15 the larger ship has moved further away from the instrument, leading for the first time in this sequence to a higher concentration on ΔL, far away from the instrument, than close by.

Figure 7 shows again in more detail the measurements, ship and plume positions from Panel 10. To highlight the entire retrieved two dimensional NO_2 field in the measurement region along the shipping lane, the four previous MAX-DOAS measurements are shown as well, which were measured between 30 seconds and 3 minutes before. The strong horizontal gradient between enhanced NO_2 concentrations close to the site and low concentrations further away for such a north wind situation is clearly visible in the figure.

Atmos. Meas. Tech. Discuss., https://doi.org/10.5194/amt-2018-348
Manuscript under review for journal Atmos. Meas. Tech.
Discussion started: 11 December 2018

4.3 Southerly wind situations

The second selected case study shows a diametrically opposite situation: For southerly winds the emitted pollution plumes are blown to the north of the shipping lane (compare Fig. 1b), further away from the instruments. As a result, NO_2 concentrations south of the shipping lane, close to the instruments, should be low, resembling situation (b) in Fig. 2. On-site in situ instruments are not able to measure the ship emission plumes.

Figure 6 shows a 12 minute sequence of consecutive measurements on 13 August 2014 starting at 12:35 UTC (14:35 local time). It shows MAX-DOAS path averaged NO_2 VMRs as well as in-situ measurements.

In the map sequence, three ships can be seen on the shipping lane, two large ones (336 m and 365 m) and a smaller one (100 m). As all ships move in the same, eastward, direction, the plume trajectories are almost parallel. Apart from the ship emission plumes, another plume crosses the area of interest, originating from the two directly adjacent coal-fired power plants in Wilhelmshaven, located at 53.57°N, 8.14°E, in a distance of about 50 km, southwest of the measurement site. Using the 10 m a.g.l. wind speed of $7.5 \pm 1.0\,\mathrm{m\,s^{-1}}$ the plume age is estimated to be around 110 minutes, and even shorter taking into account that wind speed increases with height.

Panel 1 shows the MAX-DOAS measurement at 12:35:31 UTC in the 310° azimuth direction. The horizontal path averaged NO_2 VMR along the UV light path is low (∼0.6 ppb) and on ΔL slightly enhanced (∼1 ppb), meaning low NO_2 close to the instrument and enhanced NO_2 further away (than the UV scattering point). The source for the enhanced NO_2 signal on ΔL could either be the small ship's plume or plumes from the more distant power plants.

The next measurement in Panel 2 at 335° azimuth gives similar results. In this viewing direction the plume of the small ship is not in the line of sight of the instrument, indicating that the plume originating from the power plants is the source of the slightly enhanced NO_2 VMR along ΔL.

In Panel 3 (5° azimuth) the MAX-DOAS instrument is measuring towards the two adjacent plumes of the two large ships, one located close to the UV scattering point and the other one further away. NO_2 VMR is high (∼2 ppb) behind the UV scattering point and medium high (∼1 ppb) closer to the instrument.

Panel 4 (35° azimuth) shows again high values far away from the instrument and medium high values close by.

In Panel 5 (65° azimuth), only one of the two plumes is in the line of sight and is further away than the UV scattering point, leading to enhanced NO_2 along ΔL and low (ambient) NO_2 along the UV path.

Panels 6 and 7 are similar to Panels 1 and 2, showing that the situation in these viewing direction has not changed four minutes later.

In Panel 8, four minutes after Panel 3, the plumes of the two big ships traveled a bit further northward, making the gradient between NO_2 VMRs on UV path and ΔL even stronger.

Panels 10 to 12 are similar to Panels 5 to 7.

In Panels 13 to 15, the plumes of the two big ships are now clearly only probed by the visible light path giving enhanced NO_2 concentrations along ΔL and low, ambient NO_2 concentrations along the UV path.

Atmos. Meas. Tech. Discuss., https://doi.org/10.5194/amt-2018-348
Manuscript under review for journal Atmos. Meas. Tech.
Discussion started: 11 December 2018

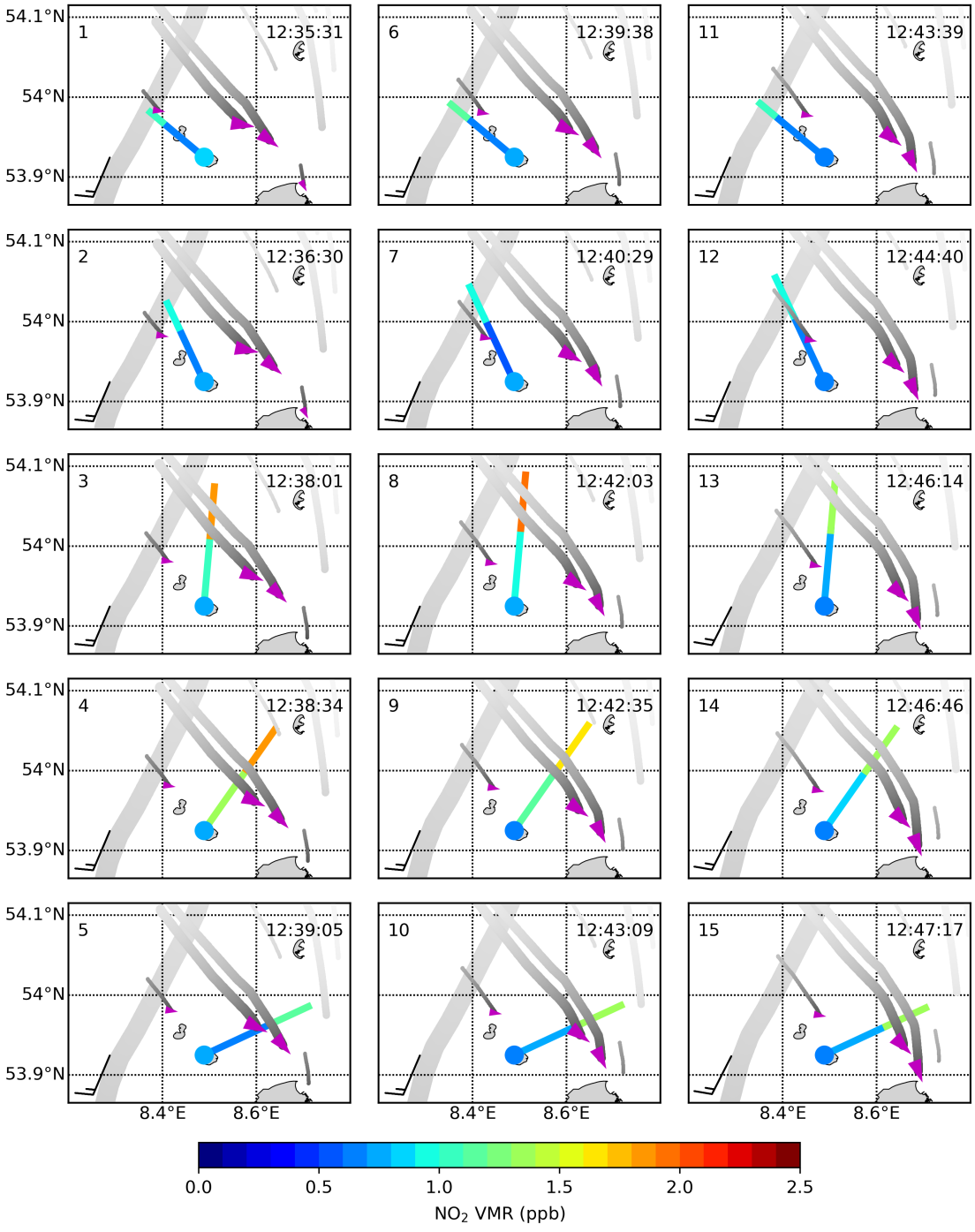

Figure 8. Sequence of maps showing 15 consecutive measurements in 0.5° elevation on 13 August 2014, starting at 12:35 UTC (14:35 local time): The extent of the UV path and ΔL and corresponding path averaged NO_2 VMRs are shown as colored lines. In situ NO_2 VMRs are shown as a colored dot at the location of the measurement site. Magenta triangles show the ship position and course (sharp tip), with larger triangles for larger ships. Gray stripes show forward trajectories of the emission plumes calculated from wind speed and direction for the moving ship. Wind direction and speed is shown with meteorological wind barbs.

Atmos. Meas. Tech. Discuss., https://doi.org/10.5194/amt-2018-348
Manuscript under review for journal Atmos. Meas. Tech.
Discussion started: 11 December 2018

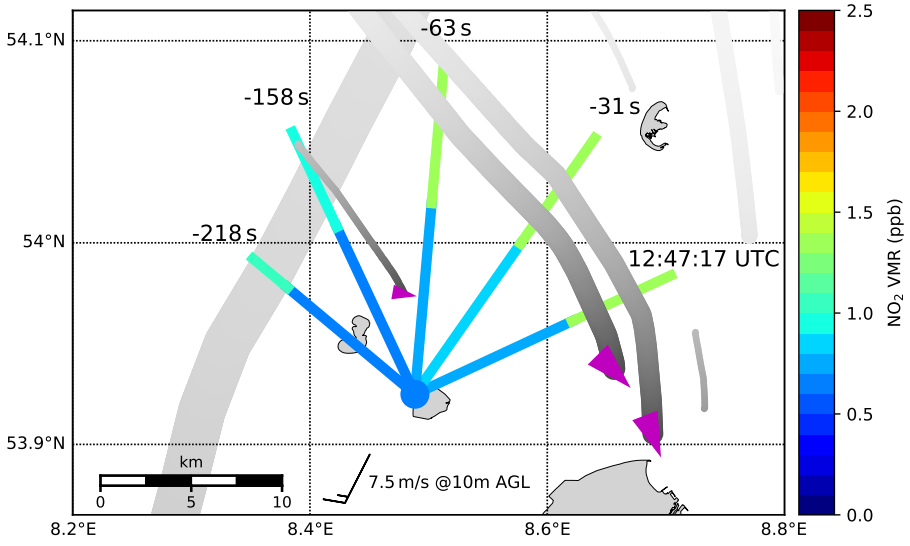

Figure 9. Map showing a zoom in onto Panel 15 of Figure 8 and also the four previous MAX-DOAS observations, being measured between 30 seconds and 3.5 minutes before the current observation. Horizontal light path lengths and corresponding path averaged volume mixing ratios of NO_2 are shown as colored lines, in situ NO_2 values as a colored dot at the location of the instrument. Magenta triangles show the ship position and course, with larger triangles for larger ships. Gray stripes show forward trajectories of the emission plumes calculated from wind speed and direction for the moving ship. The broader plume in the eastern part of the map originates from the Wilhelmshaven power plants. Please keep in mind that ship and plume position were different for the past measurements. Wind direction and speed is shown with a meteorological wind barb.

In all 15 consecutive measurements shown in the map sequence the in situ instrument measured constantly low values. This indicates that for southerly winds it cannot detect ship emission plumes at this site. Measured NO_2 VMRs agree very well with ambient NO_2 VMRs from the MAX-DOAS, retrieved south of the shipping lane along the UV path.

Figure 9 shows again in more detail the measurements, ship and plume positions from Panel 15. To highlight the entire retrieved two dimensional NO_2 field in the measurement region along the shipping lane, the four previous MAX-DOAS measurements are shown as well, being measured between 30 seconds and 3.5 minutes before. It highlights the horizontal gradient between low NO_2 concentrations close to the site and enhanced concentrations further away, northward of the shipping lane, demonstrating that with MAX-DOAS it is well feasible to measure ship emission plumes under conditions unfavorable for in situ measurements.

Atmos. Meas. Tech. Discuss., https://doi.org/10.5194/amt-2018-348
Manuscript under review for journal Atmos. Meas. Tech.
Discussion started: 11 December 2018

Atmospheric Measurement Techniques Discussions

5 Comparison of NO_2 VMRs retrieved from MAX-DOAS with airborne imaging DOAS measurements during the NOSE campaign 2013

To validate the onion peeling MAX-DOAS approach, the NO_2 VMRs retrieved from the MAX-DOAS measurements have been compared to other, independent measurements. As already indicated above, the comparison to on-site in situ trace gas analyzers is well suited for ambient NO_2 background values or specific constellations, but fails for in-plume concentrations in many constellations. For unfavorable wind conditions, like southerly winds, the in situ instrument does not detect the plumes at all. The spatial resolution of satellite instruments is not sufficient to resolve individual ship plumes, even with the newest Sentinel 5 precursor satellite ($3.5 \times 7\,km^2$, Veefkind et al. 2012). Airborne imaging DOAS measurements are the ideal method to compare to, at least on a campaign base, since they can deliver high resolution NO_2 maps along the azimuthal viewing directions of the instrument. Such measurement have been performed during the NOSE (for german "Nord-Ost-See-Experiment" meaning "North and Baltic sea experiment") campaign on 21 August 2013.

5.1 AirMAP instrument and data analysis

The Airborne imaging Differential Optical Absorption Spectroscopy instrument for Measurements of Atmospheric Pollution (AirMAP) is a push-broom imaging DOAS instrument. Scattered sunlight from below the aircraft is collected by a wide-angle objective and coupled into a sorted bundle of 35 sorted optical fibers. The image of the vertically stacked fibers is then dispersed by an imaging grating spectrometer and mapped onto a frame-transfer-CCD. The field of view of around 52° leads to a ground swath width similar to the flight altitude. With this set-up, 35 across track pixels are measured simultaneously with an exposure time of 0.5 seconds, leading to a spatial resolution better than 50 m when the aircraft is flying at 1600 m altitude. For more detailed information on the instrument see Schönhardt et al. (2015) and Meier et al. (2017).

Differential slant column densities of NO_2 were retrieved in a fit window of 425-450 nm using the settings described in Meier et al. (2017). For the retrieval of NO_2 vertical column densities, air mass factors were calculated for an NO_2 box profile in the lowest 500 m, in an atmosphere without aerosols and for a constant surface reflectance of 0.05.

5.2 NOSE campaign 2013

The NOSE campaign took place in northern Germany in August 2013 aiming at the measurement of shipping emissions in support of the MESMART project. On 21 August between 9:00 and 12:30 UTC a flight over the Neuwerk region was performed with a flight pattern covering the individual MAX-DOAS azimuthal viewing directions. In addition to that, a low level flight over an individual ship following the emitted plume was performed. For more detailed information on the NOSE campaign see Meier (2018).

Atmos. Meas. Tech. Discuss., https://doi.org/10.5194/amt-2018-348
Manuscript under review for journal Atmos. Meas. Tech.
Discussion started: 11 December 2018

Atmospheric Measurement Techniques Discussions

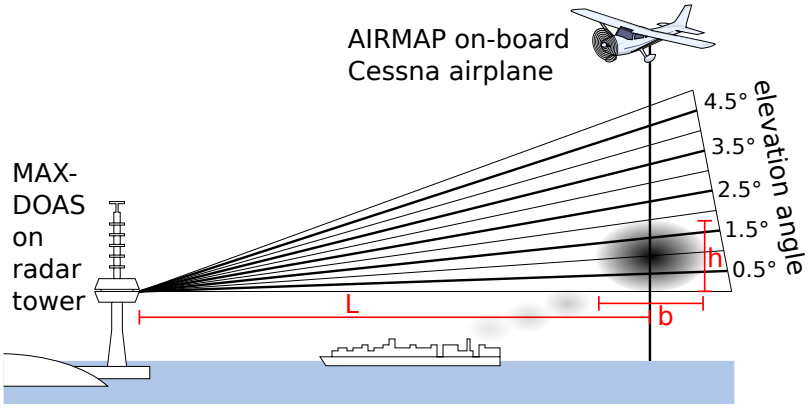

Figure 10. Sketch of the different measurement geometries of ground-based MAX-DOAS and airborne imaging DOAS instrument when measuring a ship plume. While the MAX-DOAS instrument scans the plume vertically, the AirMAP instrument measures in nadir direction. Distances and sizes are not up to scale.

5.3 Comparison between MAX-DOAS and AirMAP

The combination of ground-based MAX-DOAS with airborne imaging DOAS measurements provides mutual benefits for the interpretation of the measurements: The combination of both methods makes it possible to derive in-plume NO_2 concentrations from each method.

The onion peeling MAX-DOAS approach delivers horizontal path averaged concentrations. As discussed in Section 3.1, ship emission plumes usually fill only a small fraction of these light path segments. The average over the path segment will therefore strongly underestimate the concentration inside the plume. To retrieve the in-plume concentration, the horizontal plume extent has to be known. AirMAP high resolution NO_2 maps can provide this information.

The AirMAP measurements deliver vertical columns of NO_2 between ground and aircraft, but no information about the vertical location of the NO_2 inside the column. By assuming a box profile for the near-ground NO_2 layer, one can derive concentrations from the vertical columns. The MAX-DOAS vertical scan can provide an estimation for the vertical extent of the plume.

The crucial differences in viewing geometries are sketched in Fig. 10. The MAX-DOAS instrument scans the plume vertically by using different elevation angles giving (slanted) horizontal transects of the plume. The AirMAP instrument, measuring in nadir direction downward from the aircraft, observes vertical transects of the plume. The plume height h can be roughly estimated from the MAX-DOAS measurements if the distance is known, while the plume position and width b can be obtained from the airborne observations. Hence, the combination of both observation geometries can be used to narrow down the plume's extent in space.

Figure 11 shows MAX-DOAS path averaged VMRs along with AirMAP vertical columns of NO_2 for a ship plume measured on 21 August 2013 around 9:53 UTC (11:53 local time). The Cessna airplane, a research aircraft of the Freie Universität

Atmos. Meas. Tech. Discuss., https://doi.org/10.5194/amt-2018-348
Manuscript under review for journal Atmos. Meas. Tech.
Discussion started: 11 December 2018

Atmospheric Measurement Techniques Discussions

Berlin, housing the AirMAP instrument flew along the 335° azimuth line of sight of the instrument crossing the shipping lane and mapping multiple ship plumes. Enhanced NO_2 is measured where the aircraft overpasses the emission plumes. The southernmost plume was also covered by the MAX-DOAS instrument's NO_2 measurement in the visible spectral range. As a result, the path averaged NO_2 VMR along ΔL shows enhanced values compared to the ambient background NO_2 measured along the UV path. The time difference between both measurements of less than 20 seconds is very small as stated in the map, especially considering the integration time of the MAX-DOAS instrument of 10 seconds. The calculated forward trajectory of this plume matches the AirMAP measurements. The plumes further north have been measured by AirMAP around 1 minute later, enough time for the wind to blow the plumes northward so that the positions do not fully coincide with the plume forward trajectories which have been calculated for the MAX-DOAS measurement time.

The calculated plume trajectory matches the AirMAP measurements very well (even better in the second example in Fig. 14) and the plume position derived from the onion peeling MAX-DOAS fits to the AirMAP measurements. These results provide confidence in the calculated plume trajectories, as well as in the onion peeling approach to detect locally enhanced NO_2 levels in the ΔL light path segment.

Figure 12a shows NO_2 VCDs from AirMAP as a function of distance to the radar tower for the flight track section shown in Fig. 11. The 35 individual viewing directions were binned to 5 (1:7, 8:14, 15:21, 22:28 and 29:35) to reduce the noise. Although additional binning would reduce the noise even further, it would also smear out the plume signal, since the flight track crosses the plume not orthogonally but at an angle of about 70°(see Fig. 11). A strong enhancement of NO_2 is observed at a distance of about 9.1 km to 10.1 km. This interval is covered by the visible light path but not the UV path, which means it is completely inside the path difference ΔL. Along the UV path NO_2 VCDs are significantly lower representing ambient background pollution. There is a slight decrease of ambient NO_2 observed along the UV path from the radar tower towards the UV scattering point. Figure 12b shows the measurements of the plume in more detail, revealing the distance shift of the plume position in the different viewing directions due to the slanted angle between flight direction and plume. The NO_2 enhancement caused by the plume is roughly Gaussian-shaped in all 5 binned viewing directions, although maximum values and peak widths differ sligthly.

The measured vertical columns are total columns between flight altitude and ground level. To retrieve the local enhancement of NO_2 inside the plume, the background (ambient) column is subtracted from the total NO_2 column:

$$\begin{aligned}\mathrm{VC}_{\mathrm{plume}} &= \mathrm{VC}_{\mathrm{total}} - \mathrm{VC}_{\mathrm{background}} \\ &= (7 \pm 1) \times 10^{15}\,\mathrm{molec\,cm^{-2}} - (2.0 \pm 0.2) \times 10^{15}\,\mathrm{molec\,cm^{-2}} \\ &= (5 \pm 1) \times 10^{15}\,\mathrm{molec\,cm^{-2}}\end{aligned}$$

The plume width b can be estimated from the measurements as $b = 500\,\mathrm{m} \pm 100\,\mathrm{m}$. The three panels in Figure 13 show the MAX-DOAS DSCDs of NO_2 for the lowest 5 elevation angles measured in the UV and visible spectral range, as well as their difference, ΔDSCD. The UV measurements in Panel (a) show the typical elevation angle dependency for tropospheric absorbers, with longest light paths (and therefore highest DSCDs) in the lowest elevation angles. When the instrument points further up (higher elevation angles), the light path lengths through the troposphere decrease giving smaller DSCDs.

Atmos. Meas. Tech. Discuss., https://doi.org/10.5194/amt-2018-348
Manuscript under review for journal Atmos. Meas. Tech.
Discussion started: 11 December 2018

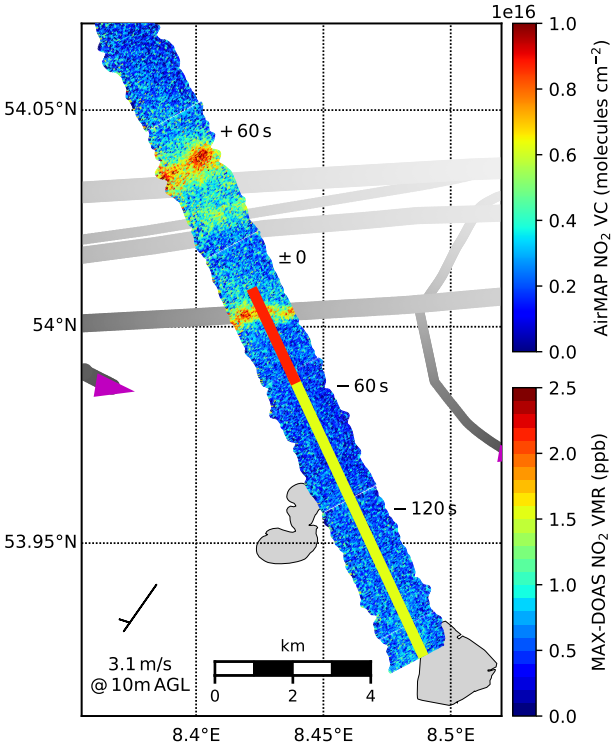

Figure 11. Map showing the MAX-DOAS path averaged VMRs (colored lines) and AirMAP vertical columns of NO_2 (broad image stripe beneath) on 21 August 2013 around 9:53 UTC (11:53 local time). As the plotted physical quantities are entirely different (VMRs and columns), color scale agreements are not expected (and completely random). Magenta triangles show current ship positions and course. Grey stripes show forward trajectories of the ship emission plumes calculated from wind speed and direction for the MAX-DOAS measurement time. The time difference between AirMAP and MAX-DOAS measurements is indicated in the map at specific parts of the flight track. Wind direction and speed is shown with a meteorological wind barb.

Comparing Panel (b), showing the visible measurements, to Panel (a), the values are in general larger due to the longer light path but show a similar separation except for the "gap" between the low elevations (0.5°, 1.5°) and higher elevations (2.5°, 3.5°, 4.5°). This implies that there is even more additional NO_2 in the lower elevations than is expected from the longer light path lengths in the visible. The gap is even more pronounced when calculating the differences between both DSCDs, shown in Panel (c). The excess NO_2 originates from the ship emission plume. Assuming that the plume vertically fills the whole vertical field of view of the 0.5° and 1.5° elevation an upper boundary for the plume height h can be calculated. The field of view of

Atmos. Meas. Tech. Discuss., https://doi.org/10.5194/amt-2018-348
Manuscript under review for journal Atmos. Meas. Tech.
Discussion started: 11 December 2018

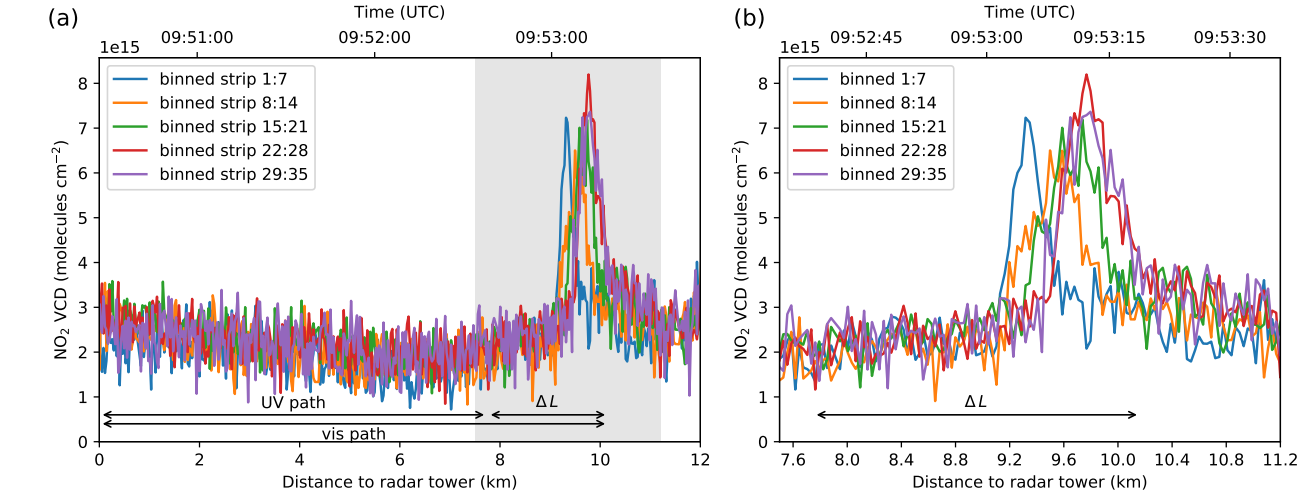

Figure 12. AirMAP vertical columns of NO_2 as a function of distance (lower axis) or time (upper axis) for the flight track section shown in Fig. 11. The right plot is a zoom in on the grey shaded area. Horizontal arrows denote the horizontal effective light paths.

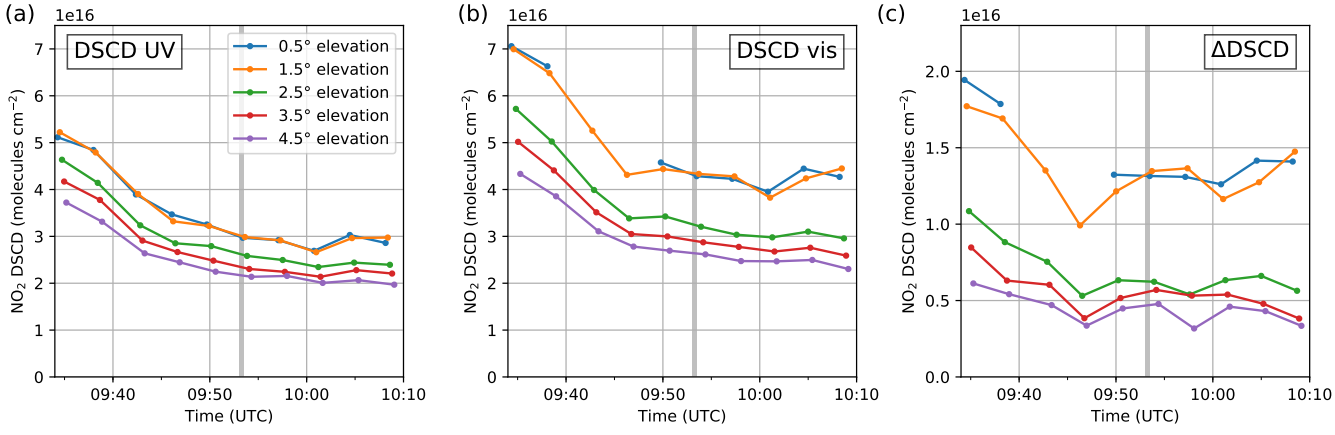

Figure 13. MAX-DOAS differential slant column densities of NO_2 in the UV (a) and visible (b) spectral range as well as their difference ΔDSDC (c) for the five lowest elevation angles for the azimuthal viewing direction of 335°. The vertical gray line indicates the AirMAP plume overpass time.

the instrument is around 1.0°. Thus the plume is observed in a solid angle of 2.0° (see Fig. 10). At a distance of 9.6 km, this corresponds to a plume height of $h = 9.6\,\mathrm{km} \cdot \tan 2° \approx 335\,\mathrm{m}$.

The plume, as can be seen in Fig. 11 and 12b, is only partly covered by the ΔL light path segment. To retrieve the in-plume NO_2 DSCD, the ambient NO_2 background within ΔL has to be subtracted. This can either be estimated from the measurements in the slightly higher elevations, which presumably do not contain plume NO_2, assuming constant NO_2 background in the lower

Atmos. Meas. Tech. Discuss., https://doi.org/10.5194/amt-2018-348
Manuscript under review for journal Atmos. Meas. Tech.
Discussion started: 11 December 2018

Atmospheric Measurement Techniques Discussions

altitudes, or from the column along the UV light path. This is not trivial, since the ambient NO_2 is not constant along this path, but increases towards the radar tower, as can be seen in Fig. 12a. Whether this slightly enhanced NO_2 is in the right height to be probed by the instruments field of view, is unknown. Either way, both estimations end up with a similar background column of $(6 \pm 1) \times 10^{15}\,\mathrm{molec\,cm^{-2}}$, the error margin reflecting the underlying uncertainty. This yields:

$$\begin{aligned}\mathrm{DSCD_{plume}} &= \Delta\mathrm{DSCD} - \mathrm{DSCD_{background}} \\ &\approx (13.3 \pm 0.2) \times 10^{15}\,\mathrm{molec\,cm^{-2}} - (6 \pm 1) \times 10^{15}\,\mathrm{molec\,cm^{-2}} \\ &= (7 \pm 1) \times 10^{15}\,\mathrm{molec\,cm^{-2}}\end{aligned}$$

The NO_2 columns measured horizontally (MAX-DOAS) and vertically (AirMAP) through the plume are different. This is expected, because the horizontal and vertical extent of the plume differ – the plume width is larger than its height. For a quantitative comparison, the NO_2 column densities of both measurements need to be converted to VMRs. With the plume height derived from MAX-DOAS measurements the NO_2 VMR inside the plume can be calculated for the AirMAP measurements:

$$\begin{aligned}\mathrm{VMR_{plume}} &= \frac{\mathrm{VC_{plume}}}{h \cdot n_{\mathrm{air}}} \approx \frac{(5 \pm 1) \times 10^{15}\,\mathrm{molec\,cm^{-2}}}{33500\,\mathrm{cm} \cdot 2.54 \times 10^{19}\,\mathrm{molec\,cm^{-3}}} \\ &= (6 \pm 1) \times 10^{-9} = (6 \pm 1)\,\mathrm{ppb}\end{aligned}$$

where n_{air} is the number density of air for the measured pressure of 1025.2 hPa and temperature of 19.2 °C.

The horizontal extent of the plume derived from the AirMAP measurements makes it possible to derive the same from MAX-DOAS measurements:

$$\begin{aligned}\mathrm{VMR_{plume}} &= \frac{\mathrm{DSCD_{plume}}}{b \cdot n_{\mathrm{air}}} \approx \frac{(7 \pm 1) \times 10^{15}\,\mathrm{molec\,cm^{-2}}}{50000\,\mathrm{cm} \cdot 2.54 \times 10^{19}\,\mathrm{molec\,cm^{-3}}} \\ &= (5.5 \pm 0.8) \times 10^{-9} = (5.5 \pm 0.8)\,\mathrm{ppb}\end{aligned}$$

These in-plume NO_2 VMRs retrieved from MAX-DOAS and AirMAP measurements agree well within their error margins.

Figure 14 presents another AirMAP overpass over several plumes from ten minutes earlier, again showing good agreement between the measured plume position and the approximate plume positions derived from the onion peeling MAX-DOAS. It shows even better how projected plume trajectories and real plume positions derived from AirMAP fit together.

6 Conclusions

The present study describes a novel application of the "onion-peeling" MAX-DOAS approach to measurements of shipping emissions to estimate the two-dimensional pollutant distribution in the strongly inhomogeneous NO_2 field over a shipping lane. The ability to probe air masses at different horizontal distances to the instrument to derive the approximate ship plume positions in the measurement area is shown on the basis of selected case studies out of the three year measurement period on the island Neuwerk. Located in the German Bight, 6–7 km south of the main shipping lane from the North sea into the river

Atmos. Meas. Tech. Discuss., https://doi.org/10.5194/amt-2018-348
Manuscript under review for journal Atmos. Meas. Tech.
Discussion started: 11 December 2018

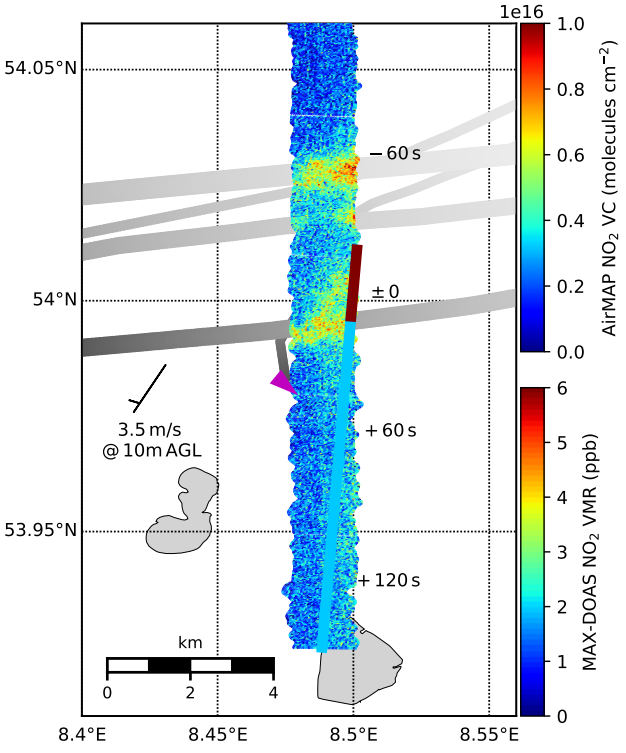

Figure 14. Map showing the MAX-DOAS path averaged VMRs (colored lines) and AirMAP vertical columns of NO_2 (broad image stripe beneath) on 21 August 2013 around 9:43 UTC (11:43 local time). As the plotted physical quantities are entirely different (VMRs and columns), color scale agreements are not expected (and completely random). Magenta triangles show current ship positions and course. Grey stripes show forward trajectories of the ship emission plumes calculated from wind speed and direction for the MAX-DOAS measurement time. The time difference between AirMAP and MAX-DOAS measurements is indicated in the map at specific parts of the flight track. Wind direction and speed is shown with a meteorological wind barb.

Elbe towards the harbor of Hamburg, the island was selected as an ideal site for the application of the onion peeling approach. It is located in a suitable distance to the shipping lane for exploiting the use of UV and visible radiation to probe the emission plumes released from the passing ships.

To determine the horizontal light path lengths for the onion peeling, a simple approach using the trace gas column of the oxygen collision complex, O_4 has been applied. To compare the measurements on the shorter UV path with the measurements on the longer visible path, horizontal path-averaged volume mixing ratios have been derived from the measured column amounts of NO_2. In addition to that, the NO_2 mixing ratio on the path difference, which was usually located over or close to

the shipping lane in our measurements, can be calculated from UV and visible measurements, providing the NO_2 concentration several kilometers away from the instrument.

For northerly wind directions, the onion peeling MAX-DOAS can detect enhanced NO_2 concentrations close to the instrument south of the shipping lane and low NO_2 concentrations north of the shipping lane. For southerly wind directions, low NO_2 values are measured close to the site south of the shipping lane and enhanced NO_2 values in the north of the shipping lane, demonstrating that the MAX-DOAS instrument can detect pollution several kilometers away from the instrument under wind directions unfavorable for in situ measurements.

A comparison to airborne imaging DOAS measurements during the NOSE campaign 2013 shows the validity of the approach. The good agreement of AirMAP measured and MAX-DOAS derived plume positions shows that MAX-DOAS measurements can be used to derive the approximate position of the emission plumes. The good agreement of plume locations calculated from wind and AIS data with the AirMAP measurements shows that simple forward trajectories provide sufficient accuracy to model the two-dimensional NO_2 field over the shipping lane. Combining airborne vertical column and ground based horizontal column measurements provides mutual benefits, enabling the independent derivation of in-plume volume mixing ratios from both measurement techniques. AirMAP and MAX-DOAS in-plume VMR agree well within their error margins, again confirming the validity of the onion peeling MAX-DOAS approach.

To conclude, the presented measurements provide a real world demonstration that the onion peeling approach works for MAX-DOAS measurments and can successfully be applied to ship emission measurements.

Data availability. The data used in this study are available from the cited references and directly from the authors upon request.

Competing interests. The authors declare that they have no conflict of interest.

Acknowledgements. The research project which facilitated the reported study was funded in part by the German Federal Maritime and Hydrographic Agency (Bundesamt für Seeschifffahrt und Hydrographie, BSH) and the University of Bremen. The authors thank the Waterways and Shipping Office Cuxhaven (Wasser- und Schifffahrtsamt, WSA), the Hamburg Port Authority (HPA), the AirMAP and NOSE teams and the FU Berlin for their help and support.

References

Alföldy, B., Lööv, J. B., Lagler, F., Mellqvist, J., Berg, N., Beecken, J., Weststrate, H., Duyzer, J., Bencs, L., Horemans, B., Cavalli, F., Putaud, J. P., Janssens-Maenhout, G., Csordás, A. P., Van Grieken, R., Borowiak, A., and Hjorth, J.: Measurements of air pollution emission factors for marine transportation in SECA, Atmospheric Measurement Techniques, 6, 1777–1791, doi:10.5194/amt-6-1777-2013, 2013.

Gomez, L., Navarro-Comas, M., Puentedura, O., Gonzalez, Y., Cuevas, E., and Gil-Ojeda, M.: Long-path averaged mixing ratios of O3 and NO2 in the free troposphere from mountain MAX-DOAS, Atmospheric Measurement Techniques, 7, 3373–3386, doi:10.5194/amt-7-3373-2014, 2014.

Hönninger, G., von Friedeburg, C., and Platt, U.: Multi axis differential optical absorption spectroscopy (MAX-DOAS), Atmos. Chem. Phys., 4, 231–254, 2004.

IMO: Safety of Life at Sea - Safety of Navigation Chapter V, Tech. rep., International Maritime Organisation (IMO), 2002.

IMO: Resolution MEPC.176(58). Amendments to the Annex of the Protocol of 1997 to Amend the International Convention for the Prevention of Pollution from Ships, 1973, As Modified By the Protocol of 1978 Relating Thereto (Revised MARPOL Annex VI)., Tech. rep., International Maritime Organisation (IMO), 2008.

Lampel, J., Pöhler, D., Tschritter, J., Frieß, U., and Platt, U.: On the relative absorption strengths of water vapour in the blue wavelength range, Atmospheric Measurement Techniques, 8, 4329–4346, doi:10.5194/amt-8-4329-2015, 2015.

Meier, A. C.: Measurements of Horizontal Trace Gas Distributions Using Airborne Imaging Differential Optical Absorption Spectroscopy, phd thesis, University of Bremen, Bremen, 2018.

Meier, A. C., Schönhardt, A., Bösch, T., Richter, A., Seyler, A., Ruhtz, T., Constantin, D. E., Shaiganfar, R., Wagner, T., Merlaud, A., Van Roozendael, M., Belegante, L., Nicolae, D., Georgescu, L., and Philip Burrows, J.: High-resolution airborne imaging DOAS measurements of NO2 above Bucharest during AROMAT, Atmospheric Measurement Techniques, 10, 1831–1857, doi:10.5194/amt-10-1831-2017, 2017.

Meller, R. and Moortgat, G. K.: Temperature dependence of the absorption cross sections of formaldehyde between 223 and 323 K in the wavelength range 225-375 nm, Journal of Geophysical Research: Atmospheres, 105, 7089–7101, doi:10.1029/1999JD901074, http://dx.doi.org/10.1029/1999JD901074, 2000.

Ortega, I., Koenig, T., Sinreich, R., Thomson, D., and Volkamer, R.: The CU 2-D-MAX-DOAS instrument - Part 1: Retrieval of 3-D distributions of NO2 and azimuth-dependent OVOC ratios, Atmospheric Measurement Techniques, 8, 2371–2395, doi:10.5194/amt-8-2371-2015, 2015.

Rozanov, V. V., Rozanov, A. V., Kokhanovsky, A. A., and Burrows, J. P.: Radiative transfer through terrestrial atmosphere and ocean: Software package SCIATRAN, Journal of Quantitative Spectroscopy and Radiative Transfer, 133, 13–71, doi:10.1016/j.jqsrt.2013.07.004, http://dx.doi.org/10.1016/j.jqsrt.2013.07.004, 2014.

Schönhardt, A., Altube, P., Gerilowski, K., Krautwurst, S., Hartmann, J., Meier, A. C., Richter, A., and Burrows, J. P.: A wide field-of-view imaging DOAS instrument for two-dimensional trace gas mapping from aircraft, Atmospheric Measurement Techniques, 8, 5113–5131, doi:10.5194/amt-8-5113-2015, 2015.

Schreier, S. F., Richter, A., Wittrock, F., and Burrows, J. P.: Estimates of free-tropospheric NO2 and HCHO mixing ratios derived from high-altitude mountain MAX-DOAS observations in the mid-latitudes and tropics, Atmospheric Chemistry and Physics, 16, 2803–2817, doi:10.5194/acp-16-2803-2016, 2016.

Serdyuchenko, A., Gorshelev, V., Weber, M., Chehade, W., and Burrows, J. P.: High spectral resolution ozone absorption cross-sections – Part 2: Temperature dependence, Atmospheric Measurement Techniques, 7, 625–636, doi:10.5194/amt-7-625-2014, 2014.

Seyler, A., Wittrock, F., Kattner, L., Mathieu-Üffing, B., Peters, E., Richter, A., Schmolke, S., and Burrows, J. P.: Monitoring shipping emissions in the German Bight using MAX-DOAS measurements, Atmospheric Chemistry and Physics, 17, 10 997–11 023, doi:10.5194/acp-17-10997-2017, 2017.

Sinreich, R., Merten, A., Molina, L., and Volkamer, R.: Parameterizing radiative transfer to convert MAX-DOAS dSCDs into near-surface box-averaged mixing ratios, Atmospheric Measurement Techniques, 6, 1521–1532, doi:10.5194/amt-6-1521-2013, 2013.

Thalman, R. and Volkamer, R.: Temperature dependent absorption cross-sections of O2-O2 collision pairs between 340 and 630 nm and at atmospherically relevant pressure., Physical chemistry chemical physics, 15, 15 371–81, doi:10.1039/c3cp50968k, http://www.ncbi.nlm.nih.gov/pubmed/23928555, 2013.

Vandaele, A. C., Hermans, C., Simon, P. C., Roozendael, M. V., Guilmot, J. M., Carleer, M., and Colin, R.: Fourier Transform Measurement of NO2 Absorption Cross-Section in the Visible Range at Room Temperature, J. Atmos. Chem., 25, 289–305, 1996.

Veefkind, J. P., Aben, I., McMullan, K., Förster, H., de Vries, J., Otter, G., Claas, J., Eskes, H. J., de Haan, J. F., Kleipool, Q., van Weele, M., Hasekamp, O., Hoogeveen, R., Landgraf, J., Snel, R., Tol, P., Ingmann, P., Voors, R., Kruizinga, B., Vink, R., Visser, H., and Levelt, P. F.: TROPOMI on the ESA Sentinel-5 Precursor: A GMES mission for global observations of the atmospheric composition for climate, air quality and ozone layer applications, Remote Sensing of Environment, 120, 70–83, doi:10.1016/j.rse.2011.09.027, http://dx.doi.org/10.1016/j.rse.2011.09.027, 2012.

Wagner, T., Apituley, A., Beirle, S., Dörner, S., Friess, U., Remmers, J., and Shaiganfar, R.: Cloud detection and classification based on MAX-DOAS observations, Atmospheric Measurement Techniques, 7, 1289–1320, doi:10.5194/amt-7-1289-2014, 2014.

Wang, Y., Li, A., Xie, P. H., Wagner, T., Chen, H., Liu, W. Q., and Liu, J. G.: A rapid method to derive horizontal distributions of trace gases and aerosols near the surface using multi-axis differential optical absorption spectroscopy, Atmospheric Measurement Techniques, 7, 1663–1680, doi:10.5194/amt-7-1663-2014, 2014.

Wittrock, F., Oetjen, H., Richter, A., Fietkau, S., Medeke, T., Rozanov, A., and Burrows, J. P.: MAX-DOAS measurements of atmospheric trace gases in Ny-Ålesund - Radiative transfer studies and their application, Atmos. Chem. Phys., 4, 955–966, 2004.

Zhang, F., Chen, Y., Tian, C., Lou, D., Li, J., Zhang, G., and Matthias, V.: Emission factors for gaseous and particulate pollutants from offshore diesel engine vessels in China, Atmospheric Chemistry and Physics, 16, 6319–6334, doi:10.5194/acp-16-6319-2016, 2016.